

# Broad-Band Bias-Current-Tuned IMPATT Oscillator for 100–200 GHz

EIJI HAGIHARA, MASAMI AKAIKE, AND KAZUYUKI YAMAMOTO

**Abstract**—Broad-band bias-current-tuned IMPATT oscillators using harmonic oscillations have been realized for the short-millimeter wavelength region (100–300 GHz). The relationship between diode and waveguide parameters (breakdown voltage, junction diameter, and waveguide cutoff frequency) to obtain broad-band tunable oscillations is investigated theoretically and experimentally. Consequently, a tuning bandwidth of 35 GHz is obtained with IMPATT oscillators in the 160-GHz band, and 30 GHz in the 200-GHz band.

## I. INTRODUCTION

IN RECENT YEARS, many workers have made considerable efforts to obtain solid-state sources in the short-millimeter and submillimeter wavelength regions, and significant progress has been achieved with IMPATT diode oscillators in these frequency bands [1]–[3].

Tunable IMPATT oscillators, one of the most important components in exploiting the higher frequency technology, have also been studied. One of the authors previously studied bias-current-tuned IMPATT oscillators and showed a way to obtain broad-band tunable oscillators in 20–90 GHz [4]. Based on this work, swept IMPATT oscillators have been manufactured in the millimeter-wave region [5].

In the short-millimeter wavelength region, a progressive trial to obtain a tunable IMPATT oscillator was made by Chao *et al.* in the *Y* band [6]. However, in order to obtain broader tunable bandwidths, further detailed theoretical and experimental investigations are still necessary.

The purpose of this paper is to obtain broad-band tunable bias-current-tuned IMPATT oscillators in the short-millimeter wave region.

Two approaches for obtaining IMPATT oscillators in the higher frequency region are possible: 1) using diodes with lower breakdown voltage [1] or 2) utilizing harmonic frequencies of oscillation [3].

Since the first method will have some upper frequency limit resulting from the difficulty in fabricating diodes with very low breakdown voltage, the second method, in which the nonlinear property of the diode is utilized, is attractive from the view point of the oscillator circuit design.

In this paper, we will present the applicability of the harmonic oscillations to the bias-current-tuned oscillators

in the short-millimeter wavelength region. First, we will point out the problems inevitably accompanied in the short-millimeter wavelength region. Then, we will discuss the relationship between oscillation characteristics and diode and waveguide parameters. Finally, we will show experimental broad-band bias-current-tuned IMPATT oscillators which have been designed based on the above discussions. (The tunable bandwidth is 35 GHz in the 160-GHz band, and 30 GHz in the 200-GHz band.)

## II. DESIGN CONSIDERATIONS

### A. Factors to be Considered

To construct broad-band IMPATT current-tuned sweep oscillators in the short-millimeter wavelength region, simultaneous oscillation of two or more harmonics and jumps in oscillation frequency should be carefully controlled.

The IMPATT diode can generate two or more harmonic frequencies due to its nonlinearities [2]. However, the transmission bandwidth of the waveguide is fairly broad, so that two or more harmonics may propagate simultaneously. In the case where two or more harmonics fall within the transmission frequency band of the waveguide, the jumps of oscillation often happen when the diode bias current is increased to raise the oscillation frequency. Jumps usually occur from the higher harmonic oscillation frequency to other lower frequency<sup>1</sup> when the lower harmonic frequency exceeds  $f_{CL}$ <sup>2</sup>. The waveguide width should be chosen so that only one harmonic frequency falls within the transmission frequency band of the waveguide. For this reason, it is necessary to investigate the relationship between  $f_{CL}$  and the oscillation characteristics to broaden the tunable bandwidth of oscillators.

### B. Diode Characteristics

Let us first discuss the selection of the breakdown voltage  $V_B$ . One of the authors previously examined the relationship between  $V_B$ , and oscillation frequency  $f$  for 20–90

<sup>1</sup>This oscillation after-jump usually differs from the bias-current-tuned oscillation. The oscillation frequency does not change with the bias current, but changes with the mechanical tuning.

<sup>2</sup>Since the fundamental mode of the rectangular waveguide is the  $TE_{01}$  mode,  $f_{CL}$  is the waveguide cutoff frequency  $f_C$ . The characteristic impedance of the waveguide changes considerably in the neighborhood of  $f_C$ . In the previous work in 20–90 GHz band,  $f_{CL}$  was given as the frequency at which the wavelength in the waveguide is twice the wavelength in the free space (that is,  $f_{CL} = 1.15 f_C$ ).

Manuscript received July 15, 1981; revised May 18, 1982.

E. Haghara and K. Yamamoto are with Yokosuka Electrical Communication Laboratory, Nippon Telegraph and Telephone Public Corporation, 1-2356, Take, Yokosuka-shi, Kanagawa-ken, 238-03, Japan.

M. Akaike is with Musashino Electrical Communication Corporation, Nippon Telegraph and Telephone Public Corporation, 3-9-11, Midori-cho, Musashino-shi, Tokyo-to, 180, Japan.

GHz IMPATT oscillators [4]. It shows that the broad-band bias-current-tuned oscillation can be obtained according to the following relationship between  $V_B$  (V) and  $f$  (GHz) as

$$2.65 \leq \log_{10} f + 0.8 \log_{10} V_B \leq 2.74. \quad (1)$$

The IMPATT diode not only generates the oscillation shown in the above equation, but also is expected to generate higher harmonics due to its nonlinearity. Fig. 1 shows a plot for harmonic frequencies above 100 GHz, using (1). The areas of (1), (2), and (3) are ones corresponding to the (1) third-, (2) fourth- and (3) fifth-harmonic oscillations, respectively. This figure predicts that broad-band oscillation can be obtained in the 200-GHz band, with the fourth harmonic, when diodes with a  $V_B$  of about 10 V are used. It also predicts that the 140-GHz band oscillation can be obtained when diodes with  $V_B \approx 10$  V (the third harmonic) or  $V_B \approx 13$  V (the fourth harmonic) are used.

In practical oscillators, the junction diameters of diodes affect the oscillation frequency, since the diode impedance is directly related to the junction capacitance. We will discuss later in the experiment the optimization of the junction diameter.

### C. Circuit Design

The previous work for 20–90 GHz shows that the stable oscillation starts at the frequency where the ratio of the guided wavelength of the  $TE_{01}$  mode to  $\lambda_0$  (free-space wavelength) is approximately 2, and that it stops at the frequency where the  $TE_{02}$ -mode cutoff attenuation is approximately  $20 \text{ dB}/\lambda_0$ .

Fig. 2 shows the frequency coverage of the rectangular waveguides for the short-millimeter wavelength region.

As the figure shows, the absolute bandwidth of the waveguide becomes broader for a higher frequency region. It means, therefore, that there exists a case where two or more harmonics can oscillate simultaneously, and jumps or instability in oscillation, as described in (1), can take place.

Fig. 3 shows an expected broad-band bias-current-tuned oscillation frequency convergence, which is obtained by combining the above two discussions about the diode breakdown voltage and waveguide dimensions. The lower and upper regions surrounded by two sets of solid lines correspond to  $3f_0$  and  $4f_0$  harmonic oscillations<sup>3</sup> described in Fig. 1 ( $5f_0$  is not considered in the figure). As described later, indeed,  $5f_0$  was not observed in our experiment.) A dotted line shows the lower limit frequency  $f_{CL}$  of the R-1800 waveguide mount. The oscillations are expected to fall within the shadowed area in Fig. 3.

Let us consider the suitable  $V_B$ , for example, when using the R-1800 waveguide mount. For lower  $V_B$  area ( $V_B = 9$ –10 V), simultaneous oscillations at  $3f_0$  and  $4f_0$  may occur. In this area,  $4f_0$  oscillation should be eliminated, in order to obtain pure  $3f_0$  oscillation. Since the oscillation frequency

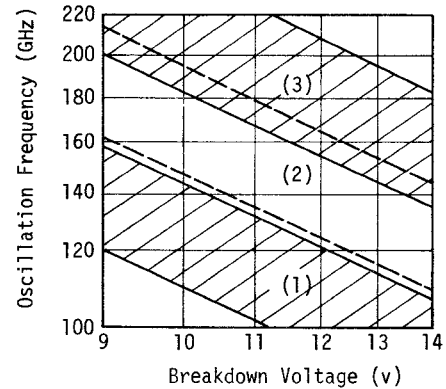


Fig. 1. Expected oscillation frequency versus breakdown voltage, corresponding to (1) the third-harmonic, (2) the fourth-harmonic, and (3) the fifth-harmonic oscillations. This figure was plotted by extending the results obtained from previous 20–90 GHz works.

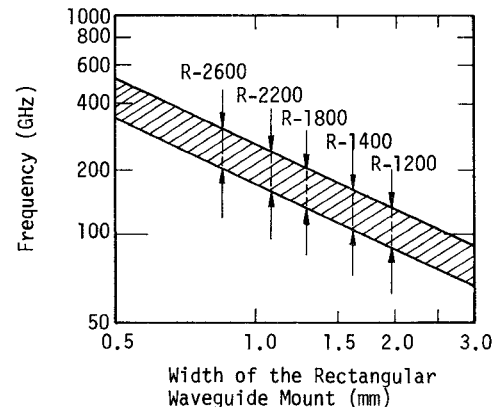


Fig. 2. Frequency coverage of the rectangular waveguide in the short-millimeter wavelength region.

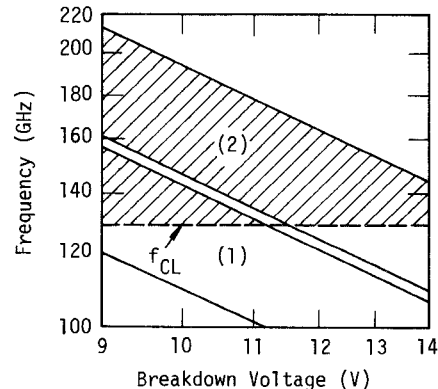


Fig. 3. Expected frequency coverage of broad-band bias-current-tuned oscillators.  $f_{CL}$  is the lower limit of the R-1800 waveguide mount.

range depends upon the diode diameter, as will be discussed later, one can achieve the  $3f_0$  oscillation only by adjusting the diode diameter. For higher  $V_B$  area ( $V_B = 12$ –14 V), only a  $4f_0$  oscillation is possible. Therefore, diodes with  $V_B \approx 10$  V and  $V_B \approx 13$  V are suitable for the R-1800 mount. Similar discussions can be given for other waveguide mounts.

In summary, frequency jump can be suppressed by selecting the suitable waveguide, the diode breakdown voltage  $V_B$ , and the diode diameter.

<sup>3</sup>In the experiment, shown in the later section, the oscillation frequency of  $(n/m) \times f_0$  ( $n/m$  ≠ integer) was not observed. Therefore, here in this paper,  $f_0$  is considered to be fundamental frequency.

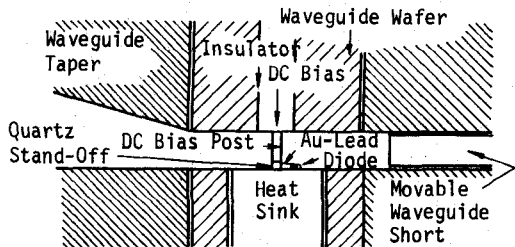


Fig. 4. A cross-sectional view of the IMPATT oscillator mount used in the experiments.

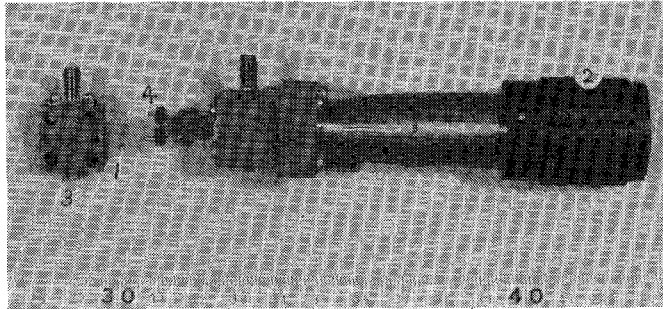


Fig. 5. A bias-current-tuned IMPATT oscillator. ① Waveguide wafer (diode mount). ② Movable short. ③ Heat sink. ④ Output taper waveguide.

### III. EXPERIMENTAL RESULTS

Experiments have been carried out to verify the preceding analysis due to the interaction among the diode and the waveguide parameters.

#### A. Structure of Oscillator

Fig. 4 shows a cross-sectional view of the IMPATT oscillator mount used in the experiments. The oscillator consists of five parts: a diode, a DC-bias post, a reduced-height rectangular waveguide, a waveguide taper, and a movable short. Fig. 5 shows the outside view of the oscillator hardware.

The diodes used here were single-drift silicon IMPATT diodes of  $p^+nn^+$  design. These diodes were fabricated from diode wafers supplied by Musashino ECL N.T.T. [7]. Fig. 6 shows an enlarged photograph and a schematic view with a scale of the IMPATT diode. The IMPATT diode chip and a quartz stand-off were bonded on a copper heat sink with thermal compression. They were connected with a gold ribbon, through which the bias current is supplied to the diode from a DC-bias post. In order to increase the oscillation frequency bandwidth, a large amount of bias current is required. Therefore, a good thermal resistance is required for reducing the junction temperature rise. Thermal resistances were measured using Haitz's method [8]. The results for the diodes with  $V_B = 13.2$  V and various diameters are shown in Fig. 7. Good agreement between the measured and the calculated values using the model given in the inset of Fig. 7 is obtained, which ensures a good thermal contact.

In the experiments for 140–260 GHz, we used the diodes with different breakdown voltages, i.e.,  $V_B = 9.6$  V, 10.0 V, 11.2 V, and 13.2 V. Different diode diameters (15  $\mu\text{m}$ –40

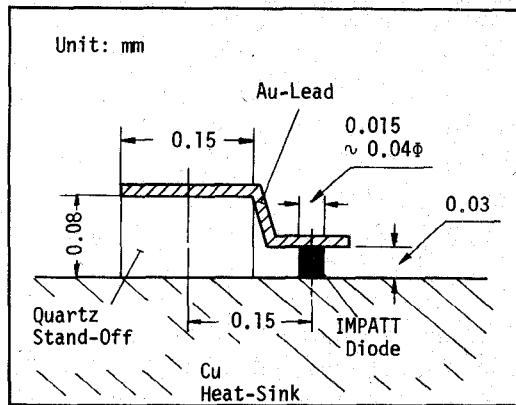
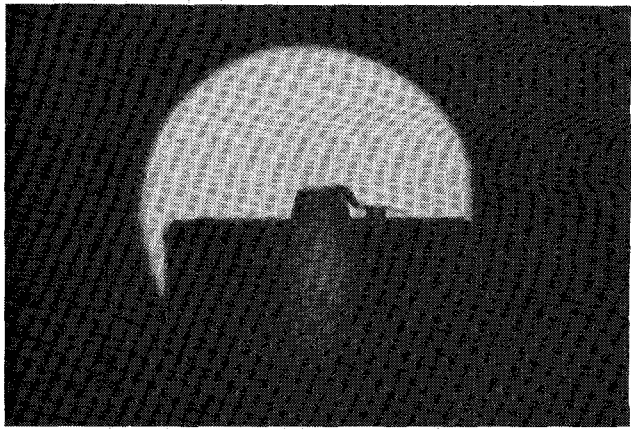


Fig. 6. An enlarged photograph and a view with a scale of an IMPATT diode.

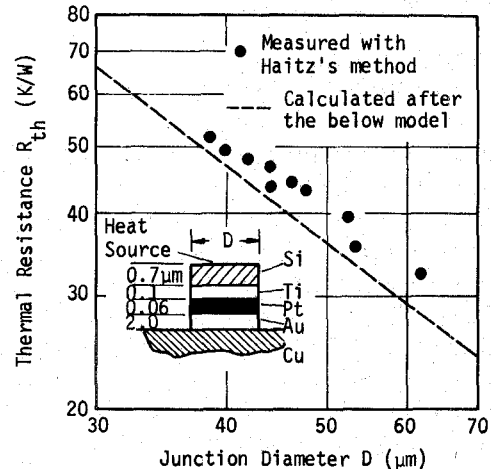


Fig. 7. Thermal resistance as a function of junction diameter of IMPATT diode.

$\mu\text{m}$ ), were also used in order to investigate the relation between the oscillation frequency and the junction diameter. They are all provided from Musashino E.C.L. [7].

Four different waveguides were used and their properties are summarized in Table I. The width of the reduced-height waveguide is the same as that of the standard one. Since the absolute value of the negative resistance of IMPATT diodes is lower than the characteristic impedance of the standard waveguide, in order to obtain a close matching between the diode and the waveguide, the height of the waveguide, within which the diode is mounted, is reduced

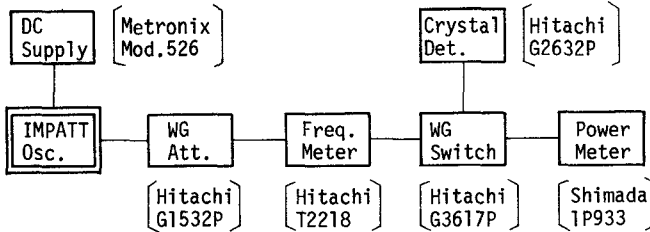


Fig. 8. Test setup for measuring RF output power and frequency of the bias-current-tuned IMPATT oscillator.

TABLE I  
WAVEGUIDES USED IN THE EXPERIMENT

Waveguide Standard	Band Width (GHz)	Size (mm)	Lower Limit Frequency $f_{CL}$ (GHz)
R-1200	90-140	2.032×0.50	84.84
R-1400	110-170	1.652×0.40	104.41
R-1800	140-220	1.295×0.30	133.11
R-2200	170-260	1.092×0.25	158.15

Accuracy of these waveguides is within 5 percent in the short-millimeter wavelength region in this experiment.

as usually done for broad-band IMPATT oscillators [4]–[6]. The height of waveguides used here was determined so that the characteristic impedance of the waveguide mounts is about  $200 \Omega$ <sup>4</sup>. (The characteristic impedance of a waveguide varies with frequency. This value is at the center frequency of the bandwidth.)

### B. Oscillation Characteristics

1) *Experimental Setup:* The test setup for measuring RF output power and frequency is shown in Fig. 8. RF output is measured by the thermoelectric mount and frequency is measured by the cavity-type wavelength meter. Attenuators are used for isolation between the oscillator and the load. The insertion loss of the length between the oscillator and the power meter is estimated to be 3 dB at 200 GHz.

2) *Effect of  $f_{CL}$ :* An oscillation frequency versus bias current is shown in Fig. 9. The breakdown voltage of the diode is 13.2 V. The oscillation frequency increases monotonically as the bias current is increased. Jumps of oscillation occur, however, from 143 GHz to 118 GHz when the bias current exceeds 218 mA.

The same diode was re-mounted in the R-1200 mount and the oscillation frequency versus bias current was measured. Two simultaneous oscillations were observed. One is in the 140-GHz band, which has the same oscillation frequency as in the R-1400 mount. Another is in the 110-GHz band. Since the ratio of two oscillation frequencies is exactly 4/3, we considered these oscillations to be the fourth- and third-harmonic oscillations, i.e.,  $4f_0$  and  $3f_0$ , respectively. Since the  $3f_0$  is equal to the  $f_{CL}$  ( $\sim 105$  GHz) of the R-1400 mount when the  $4f_0$  is 143 GHz, it can

<sup>4</sup>The value of  $200 \Omega$  was determined by the mechanical tolerance of the waveguide and the short-plunger.

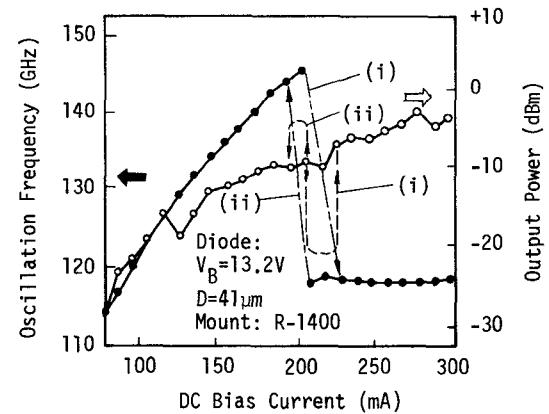


Fig. 9. Jumps in oscillation frequency. The frequency and output power have hysteresis loops around the 218 mA of dc current. The route (i) corresponds to increasing bias current, and the route (ii) corresponds to decreasing bias current.

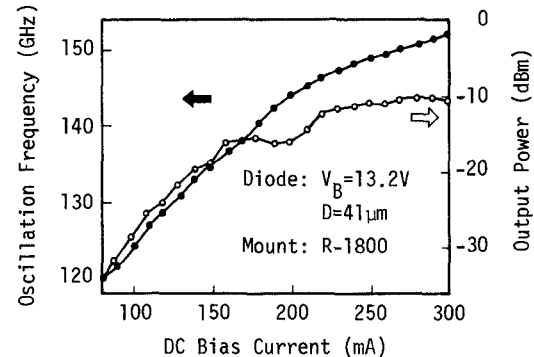


Fig. 10. Stable and broad-band bias current tuned oscillation characteristics realized by the R-1800 mount. The diode used here is the same one in Fig. 9. Undesired lower harmonic oscillation is eliminated by using the proper waveguide width.

be concluded that the  $4f_0$  oscillation jumped to the other frequency<sup>5</sup> just when the  $3f_0$  exceeds  $f_{CL}$  and begins to oscillate.

Fig. 10 shows oscillation characteristics when the R-1800 waveguide mount is used for the same diode as described in Fig. 9. The frequency varies continuously as the bias current is varied. The tuning bandwidth is more than 30 GHz. No jump of oscillation nor simultaneous oscillation was observed. Figs. 3, 9, and 10 show that undesired lower harmonic oscillation is eliminated by using the R-1800 waveguide. We can conclude, therefore, that the R-1800 waveguide is suitable for this case.

Similarly, broad-band and stable oscillations in the 160-GHz band and the 200-GHz band are shown in Figs. 11 and 12, respectively. Tuning bandwidths of 35 GHz with output power of  $-5 \sim -30$  dBm have been obtained in the 160-GHz band and 30 GHz with  $0 \sim -30$  dBm in the 200-GHz band.

3) *Effect of  $V_B$ :* Fig. 13 shows oscillation frequencies with the various diode breakdown voltages and waveguide

<sup>5</sup>This oscillation obtained after the jump differs from the bias-current-tuned oscillation. The oscillation frequency does not vary with bias current, but varies with mechanical tuning, for example, with a short-plunger.

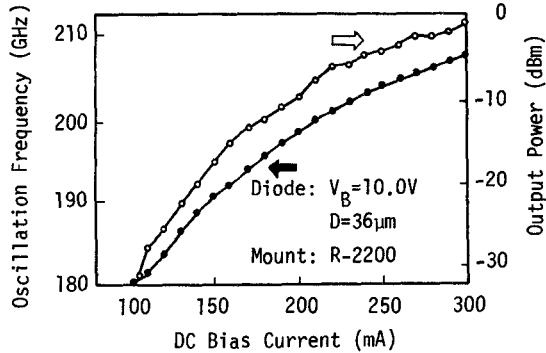


Fig. 11. Broad-band bias-current-tuned oscillation characteristics in 160-GHz band.

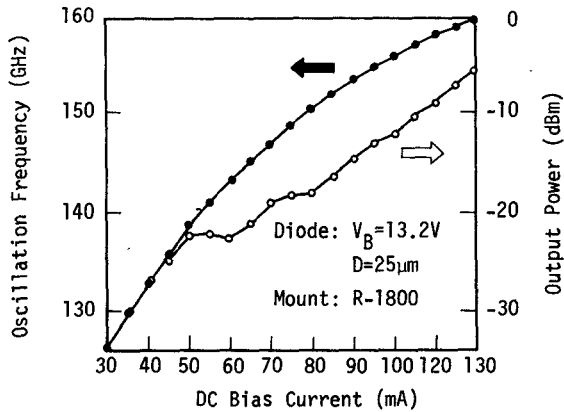


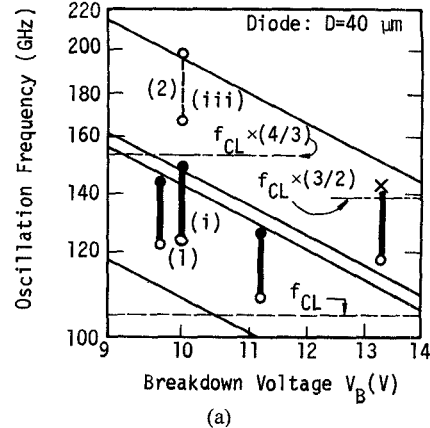
Fig. 12. Broad-band bias-current-tuned oscillation characteristics in 200-GHz band.

mounts. Regions (1) and (2) are taken from Fig. 1. Dotted lines correspond to the lower frequency  $f_{CL}$  of the waveguides. From Fig. 13(a) and (b), one can find that broad bandwidths can be obtained at 140-GHz band by using the diode with  $V_B = 10$  V and the diode with  $V_B = 13.2$  V, which correspond to the third- and fourth-harmonic oscillations, respectively. From Fig. 13(c),  $V_B = 10$  V corresponds to the fourth harmonic for the 200-GHz band. Let us compare (i) in Fig. 13(a) and (ii) in Fig. 13(b). From (i) and (ii), we know that the same oscillation frequency ranges are obtained with different  $V_B$  by selecting the suitable number of harmonic frequency and  $f_{CL}$ .

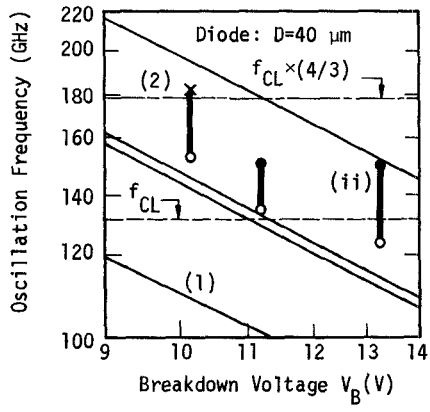
Fig. 13 suggests that the results obtained for lower frequency band (20–90 GHz) can be expanded to the short-millimeter wavelength region.

4) *Effect of Junction Diameter*: Bias-current-tuned oscillation frequency as a function of junction diameter of the diode is shown in Fig. 14. The diode with  $V_B = 13.2$  V is mounted on the (a) R-1200, (b) R-1400, and (c) R-1800 waveguide mounts. The initial diode diameter is 40  $\mu$ m. The oscillation characteristics were examined for the different waveguide mounts with the same diode. Then the diode is chemically etched to smaller diameter, and then remounted with four waveguide mounts. Four different diameters were tested.

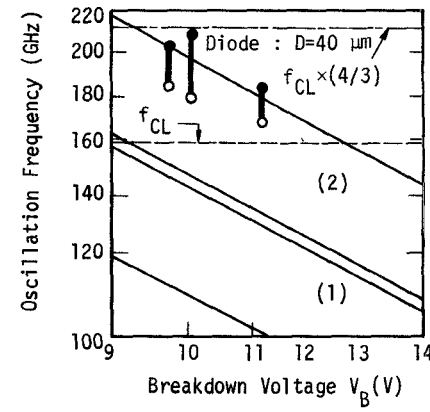
These figures show that the oscillation frequency increases as the junction diameter increases. By adjusting the



(a)



(b)



(c)

Fig. 13. Tuning frequency ranges of bias-current-tuned IMPATT oscillators in harmonic-mode operation. (1) and (2) correspond to the (1) third- and (2) fourth-harmonic oscillation, respectively. Dotted lines of (a), (b), and (c) show the lower limit frequencies of (a) R-1400, (b) R-1800, and (c) R-2200 waveguides, respectively. (○: oscillation begins, ×: jump occurs, ●: limited from thermal restriction.) From (i) and (ii), we know that the same oscillation frequency ranges are obtained with different  $V_B$  by selecting the suitable number of harmonic frequency and  $f_{CL}$ . The oscillation denoted by (iii) was eliminated by trimming the junction diameter. After trimming, only the oscillation denoted by (i) was observed.

diameter, trimming of the oscillation frequency is also possible.

5) *Effect of External Circuit*: Fig. 15 shows oscillation characteristics as a function of position of the short-plunger behind the diode. In the bias-current-tuned oscillators, it

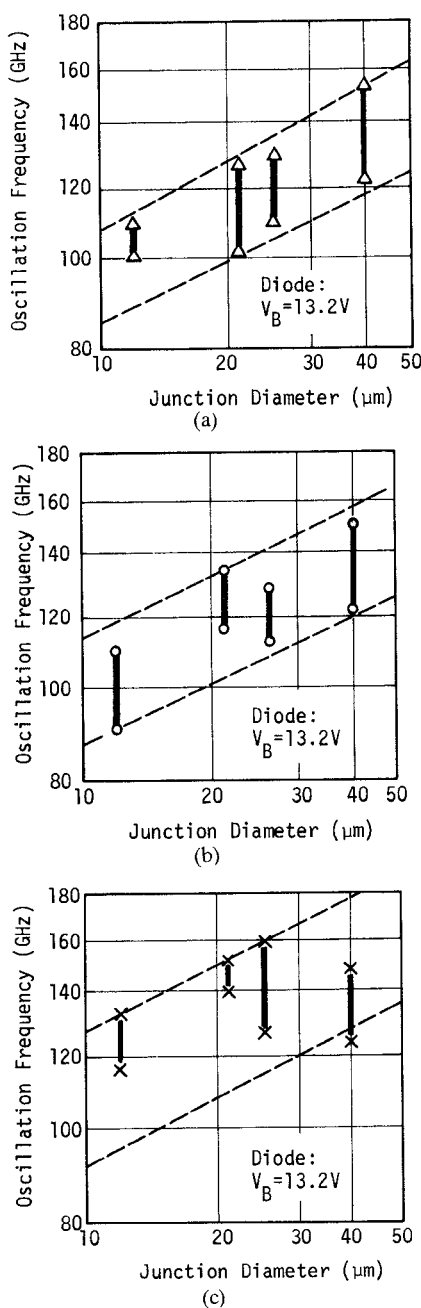


Fig. 14. Tuning frequency ranges of bias-current-tuned IMPATT oscillators with various junction diameters. Dotted lines in the figures show the trend curves. Oscillation with (a) R-1200 mount, (b) R-1400 mount, and (c) R-1800 mount.

has been found that the output power changes with the position of the short-plunger; however, the oscillation frequency remains unchanged.

#### IV. CONCLUSIONS

Bias-current-tuned IMPATT oscillators in the short-millimeter wavelength region have been described.

The relationship between oscillation frequencies and various parameters of IMPATT diodes and waveguides was discussed for optimum circuit design in the short-millimeter wavelength region. It is found that the relationship between  $f$  and  $V_B$ , which has been obtained in the millime-

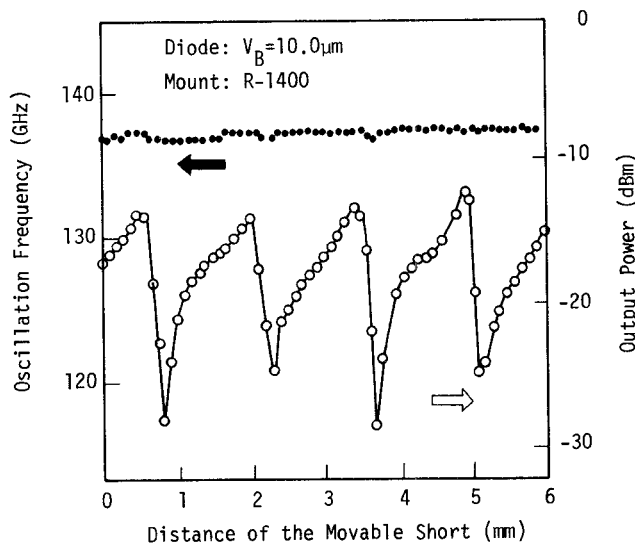


Fig. 15. Mechanical-tuned characteristics at 137 GHz as a function of distance of the movable short stub.

ter-wavelength region, can be extended in the short-millimeter wavelength region utilizing harmonic oscillations. It is also found that there are several  $V_B$ 's to obtain one  $f$ , and that jumps or undesired oscillations can be suppressed by selecting  $f_{CL}$  as well as  $V_B$  and  $d$ .

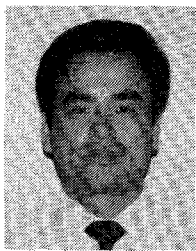
Oscillation characteristics have been experimentally investigated by constructing bias-current-tuned oscillators for 100–200-GHz range. Tuning bandwidths of 35 GHz have been obtained in the 160-GHz band and 30-GHz band in the 200-GHz band.

#### ACKNOWLEDGMENT

The authors wish to thank Dr. Yamamoto for his continuous encouragements and Dr. Ohmori for offering the IMPATT diode wafers.

#### REFERENCES

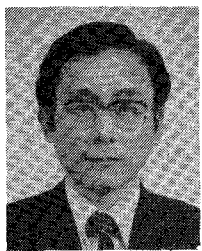
- [1] T. Ishibashi and M. Ohmori, "200-GHz 50-mW CW oscillation with silicon SDR IMPATT diodes," *IEEE Trans. Microwave Theory Tech.*, vol. MTT-24, pp. 858–859, Nov. 1976.
- [2] M. Ohmori, T. Ishibashi, and S. Ono, "Dependency of the highest harmonic oscillation frequency on junction diameter of IMPATT diodes," *IEEE Trans. Electron Devices*, vol. ED-24, pp. 1323–1329, Dec. 1977.
- [3] T. Ishibashi, M. Ino, F. Makimura, and M. Ohmori, "Liquid-nitrogen-cooled submillimeter-wave silicon IMPATT diodes," *Electron. Lett.*, vol. 13, pp. 299–300, May 1977.
- [4] M. Akaike, H. Kato, and S. Yuki, "Oscillation characteristics of millimeter-wave IMPATT diodes mounted in low-impedance waveguide mounts," *IEEE Trans. Microwave Theory Tech.*, vol. MTT-24, pp. 147–151, Mar. 1976.
- [5] S. Yuki, H. Kato, M. Akaike, and K. Kaneko, "Millimeter-wave sweep oscillator and insertion and reflection loss meter," *Rev. Elec. Commun. Lab.*, vol. 25, pp. 958–983, Sept.–Oct. 1977.
- [6] C. Chao, R. L. Bernick, E. M. Nakaji, R. S. Ying, K. P. Weller, and D. H. Lee, "Y-band (170–260-GHz) tunable CW IMPATT diode oscillators," *IEEE Trans. Microwave Theory Tech.*, vol. MTT-25, pp. 985–991, Dec. 1977.
- [7] K. Suzuki, "Millimeter-wave Si IMPATT diodes," *Rev. Elec. Commun. Lab.*, vol. 23, pp. 948–959, July–Aug. 1975.
- [8] R. H. Haitz, H. L. Stover, and N. J. Tolar, "A method for heat flow resistance measurements in avalanche diodes," *IEEE Trans. Electron Devices*, vol. ED-16, pp. 438–444, May 1969.



**Eiji Hagihara** was born in Yokkaichi, Japan, in 1950. He received the B.S. and M.S. degrees in applied physics from Nagoya University, Nagoya, Japan, in 1973 and 1975, respectively.

He joined Yokosuka Electrical Communication Laboratory, Japan, in 1975, and has been engaged in the research of millimeter-wave solid-state circuits and millimeter-wave integrated circuits. He is now a Manager at the Kinki Telecommunication Bureau, Nippon Telegraph and Telephone Public Corporation, Osaka, Japan.

Mr. Hagihara is a member of the Institute of Electronics and Communication Engineers of Japan.



**Masami Akaike** was born in Kamakura-shi, Kanagawa-ken, Japan, on October 15, 1940. He received the B.S., M.S., and Ph.D. degrees from the University of Tokyo, Tokyo, Japan, in 1964, 1966, and 1969, respectively.

He joined the Musashino Electrical Communication Laboratory, Nippon Telegraph and Telephone Public Corporation, Tokyo, Japan, in 1969. He was engaged in the research of millimeter-wave solid-state circuits and the development and design of repeaters and measuring equipment.

ments for a guided millimeter-wave transmission system. He is currently a Chief of the INS Model Development Division, Musashino Electrical Communication Laboratory, NTT.

Dr. Akaike is a member of the Institute of Electronics and Communication Engineers of Japan, and was a recipient of the 1971 IECEJ Yonezawa Memorial Scholarship.



**Kazuyuki Yamamoto** was born in Kyoto, Japan, on July 13, 1946. He received the B.S., M.S., and Ph.D. degrees in electrical engineering, from the University of Kyoto, Japan, in 1969, 1971, and 1982, respectively.

Since joining the Electrical Communication Laboratory, Nippon Telegraph and Telephone Public Corporation, Tokyo, Japan, in 1971, he has been engaged in the research and development of filters, solid-state circuits, and transmission lines for millimeter and submillimeter wavelength regions. He is currently a Staff Engineer of the Radio Transmission Section, Integrated Transmission System Development Division, Yokosuka Electrical Communication Laboratory, NTT.

Mr. Yamamoto is a member of the Institute of Electronics and Communication Engineers of Japan.

## Broad-Band Characteristics of EHF IMPATT Diodes

LOWELL H. HOLWAY, JR. AND SHIOU LUNG CHU

**Abstract**—Measurements have been made of the oscillator characteristics when a GaAs EHF double-drift IMPATT diode designed for a frequency of 35 GHz is operated over an extended frequency range from 33–50 GHz. The diode which was designed for 35 GHz has a broad-band capability which allows it to produce 2.15 W at 44.1 GHz. An analytic model is shown to predict accurately the observed results. The model indicates that the upper limit in frequency can be increased by reducing the diode area or the series resistance as well as by reducing the length of the drift region.

### I. INTRODUCTION

THE BROAD-BAND characteristics of IMPATT diodes make them a flexible power source for use in many applications. In this paper we describe a theoretical

and experimental study of the power output of a GaAs double-drift diode designed for 35 GHz when it is operated over an extended frequency range from 33–50 GHz.

The diode was operated in a top-hat circuit in which the circuit parameters were varied in order to optimize the output power at a given frequency and dc-current level. The experimental results are compared with calculations based on an analytic model described previously [1]–[4]. This analytic model uses the Read equation to describe the time behavior of the avalanche zone and assumes that the saturation current is small, that ionization in the drift region is negligible, and that the carriers move at saturated velocities. One of the important parameters of the model is the series resistance. In these calculations, we use values measured accurately by a method described elsewhere [5]. The calculated results of the model were then in close agreement with the experimental results. This model allows

Manuscript received April 7, 1982; revised June 21, 1982.

The authors are with the Raytheon Research Division, 131 Spring Street, Lexington, MA 02173.